nature astronomy

SUPPLEMENTARY INFORMATION

https://doi.org/10.1038/s41550-019-0900-2

In the format provided by the authors and unedited.

Regenerative water sources on surfaces of airless bodies

Cheng Zhu[1,2], Sándor Góbi[1,2,6], Matthew J. Abplanalp[1,2], Robert Frigge[1,2], Jeffrey J. Gillis-Davis[3*], Gerardo Dominguez[4], Katarina Miljković[5] and Ralf I. Kaiser[1,2*]

[1]Department of Chemistry, University of Hawai'i at Mānoa, Honolulu, HI, USA. [2]W.M. Keck Laboratory in Astrochemistry, University of Hawai'i at Mānoa, Honolulu, HI, USA. [3]Hawai'i Institute of Geophysics and Planetology, University of Hawai'i at Mānoa, Honolulu, HI, USA. [4]Department of Physics, California State University San Marcos, San Marcos, CA, USA. [5]School of Earth and Planetary Science, Space Science and Technology Centre, Curtin University, Perth, Western Australia, Australia. [6]Present address: Department of Chemistry, University of Coimbra, Coimbra, Portugal. *e-mail: gillis@higp.hawaii.edu; ralfk@hawaii.edu

Supplementary information for

Regenerative water sources on surfaces of airless bodies

Cheng Zhu[1,2], Sándor Góbi[1,2,†], Matthew J. Abplanalp[1,2], Robert Frigge[1,2], Jeffrey J. Gillis-Davis[3*], Gerardo Dominguez[4], Katarina Miljković[5], Ralf I. Kaiser[1,2*]

[1]Department of Chemistry, University of Hawaii at Mānoa, Honolulu, HI 96822.
[2]W.M. Keck Laboratory in Astrochemistry, University of Hawaii at Mānoa, Honolulu, HI 96822.
[3]Hawai'i Institute of Geophysics and Planetology, University of Hawai'i at Mānoa, Honolulu, HI 96822.
[4]Department of Physics, California State University, San Marcos, San Marcos, California 92096-0001, USA
[5]School of Earth and Planetary Science, Space Science and Technology Centre, Curtin University, Perth, WA, 6845, Australia
[†]Present address: Department of Chemistry, University of Coimbra, 3004–535, Coimbra, Portugal.

*Corresponding author: Jeffrey J. Gillis-Davis, gillis@higp.hawaii.edu, Ralf I. Kaiser, ralfk@hawaii.edu

The file includes:

Supplementary Figs. 1-8

Supplementary Tables 1-3

References 1-2

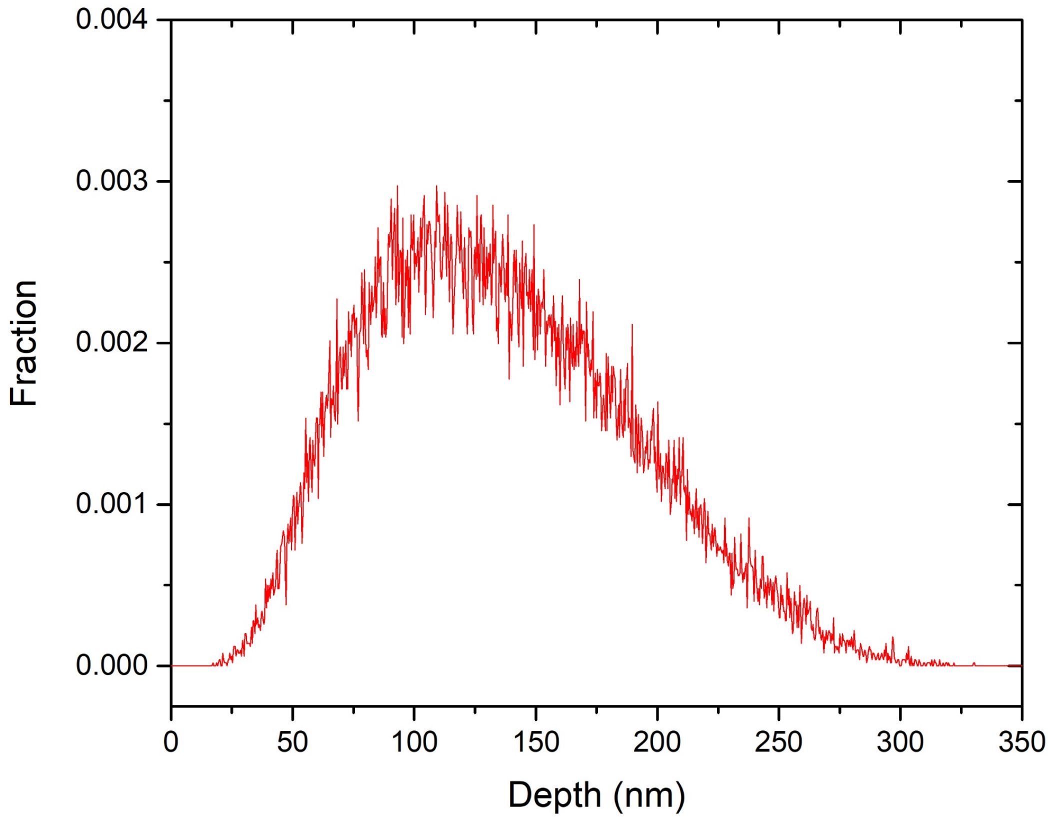

Supplementary Fig. 1. Depth implantation profile of 5 keV electrons into samples of the Murchison meteorite computed via the Casino program.

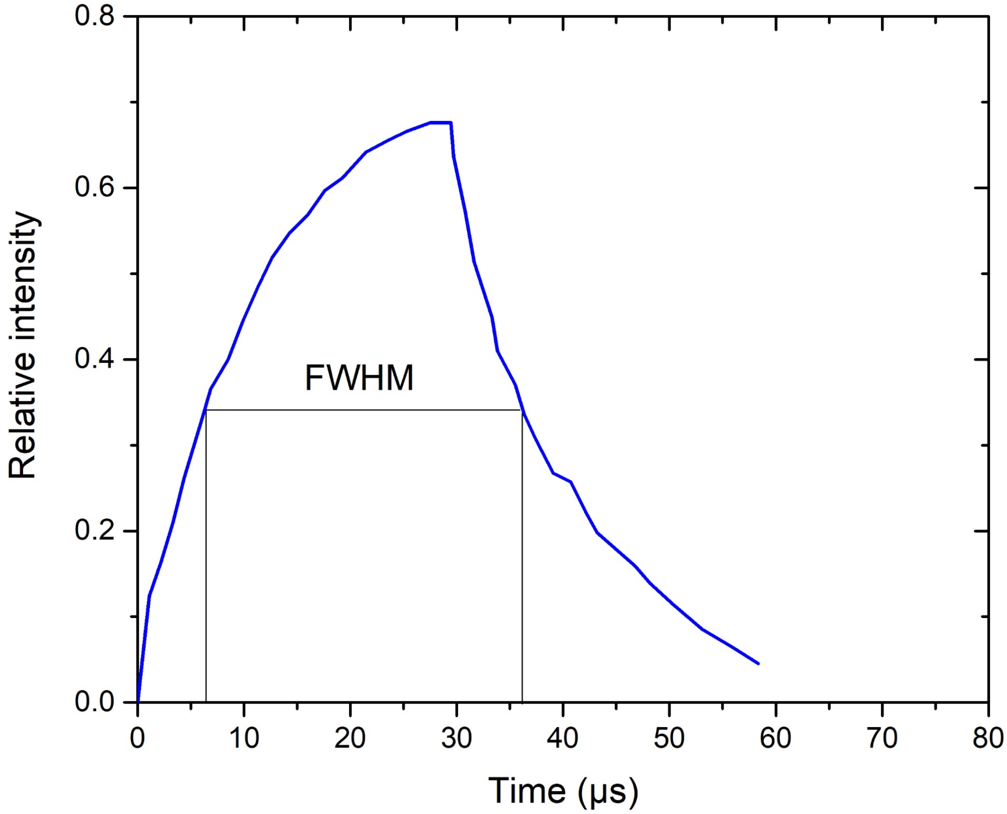

Supplementary Fig. 2. Optical output pulse (14% duty cycle at 5 kHz).

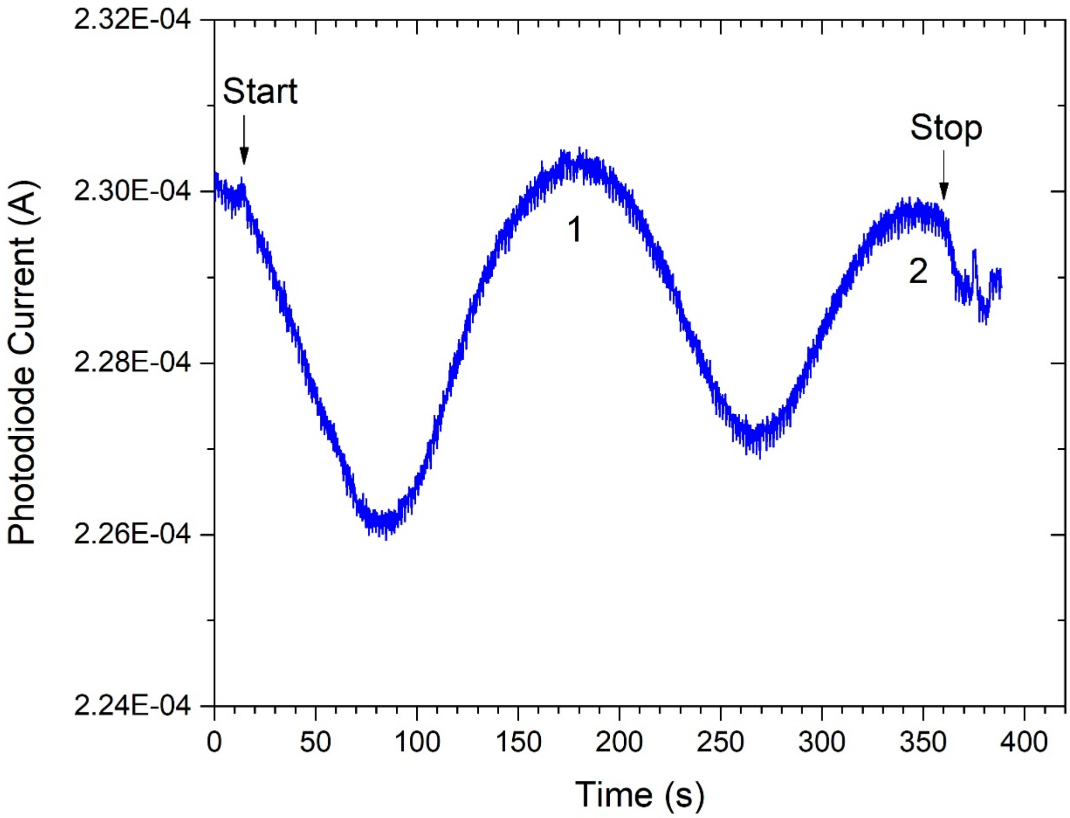

Supplementary Fig. 3. Interference plot recorded during ice deposition. Integer numbers of fringes are labeled below signal maxima, and at the deposition stop time, 2.05 fringes had accumulated.

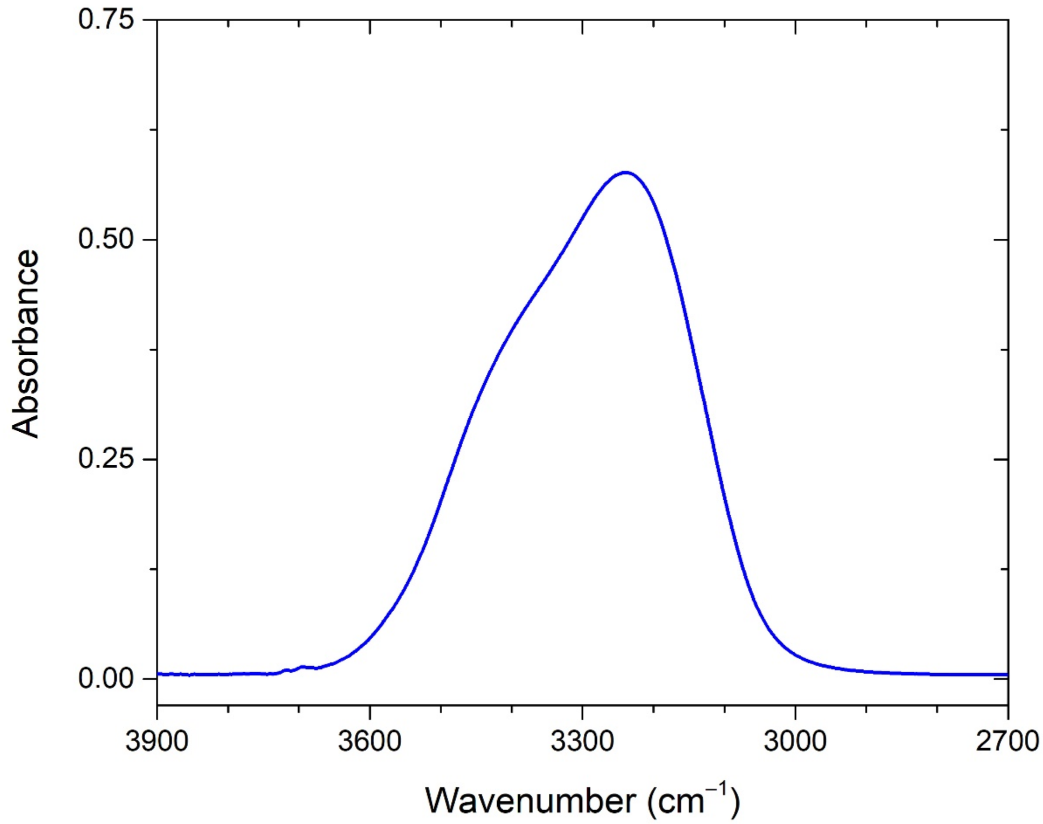

Supplementary Fig. 4. IR spectrum (O−H stretching mode) of the water ice.

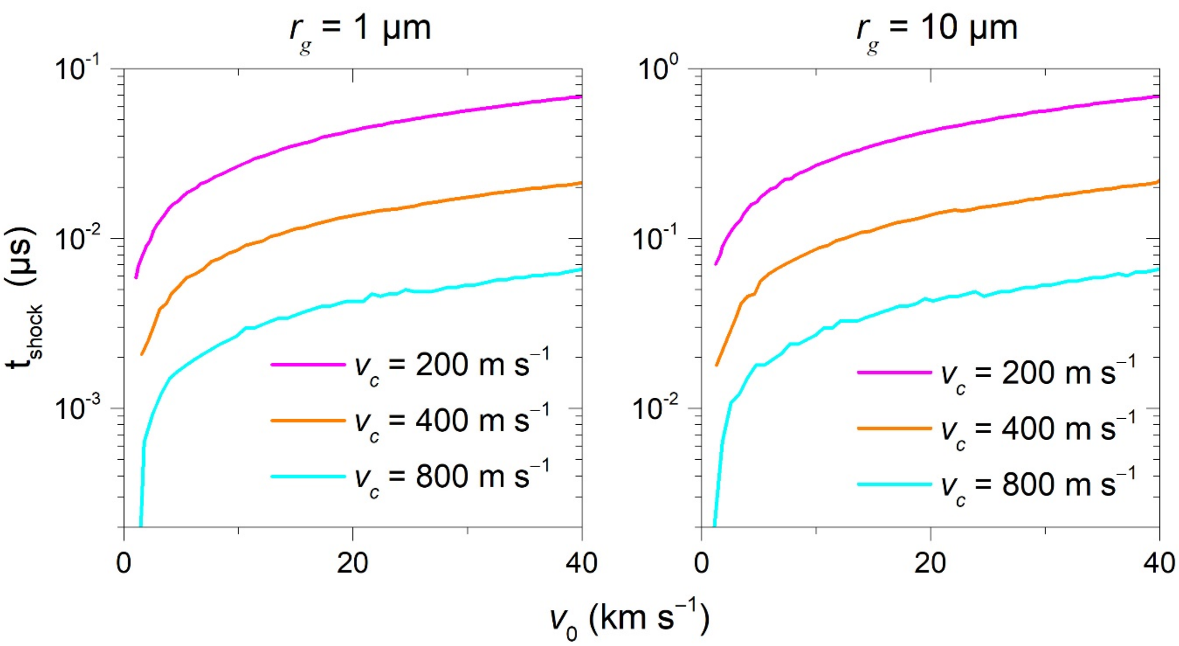

Supplementary Fig. 5. Timescales of initial shock heating resulting from micrometeorite impacts for different projectile sizes r_g, velocities v_0, and critical shock velocities v_c (Method 1).

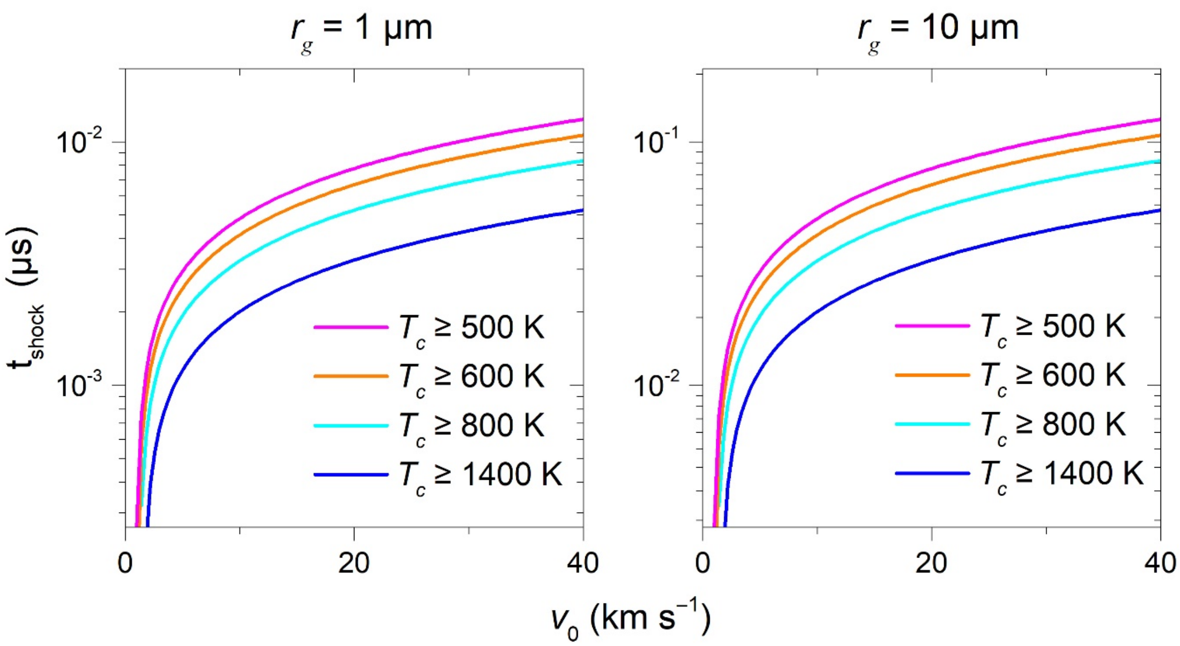

Supplementary Fig. 6. Timescales of initial shock heating resulting from micrometeorite impacts for different projectile sizes r_g, velocities v_0, and average temperature of crater T_c (Method 2).

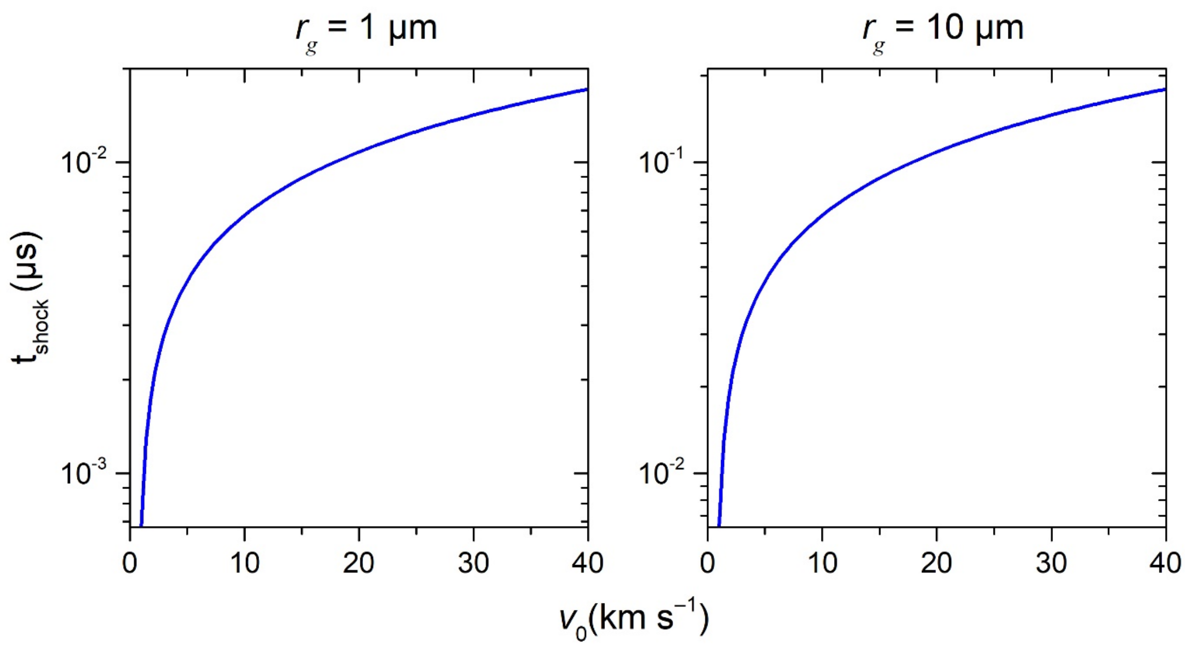

Supplementary Fig. 7. Timescales of initial shock heating resulting from micrometeorite impacts for different projectile sizes r_g and velocities v_0 (Method 3).

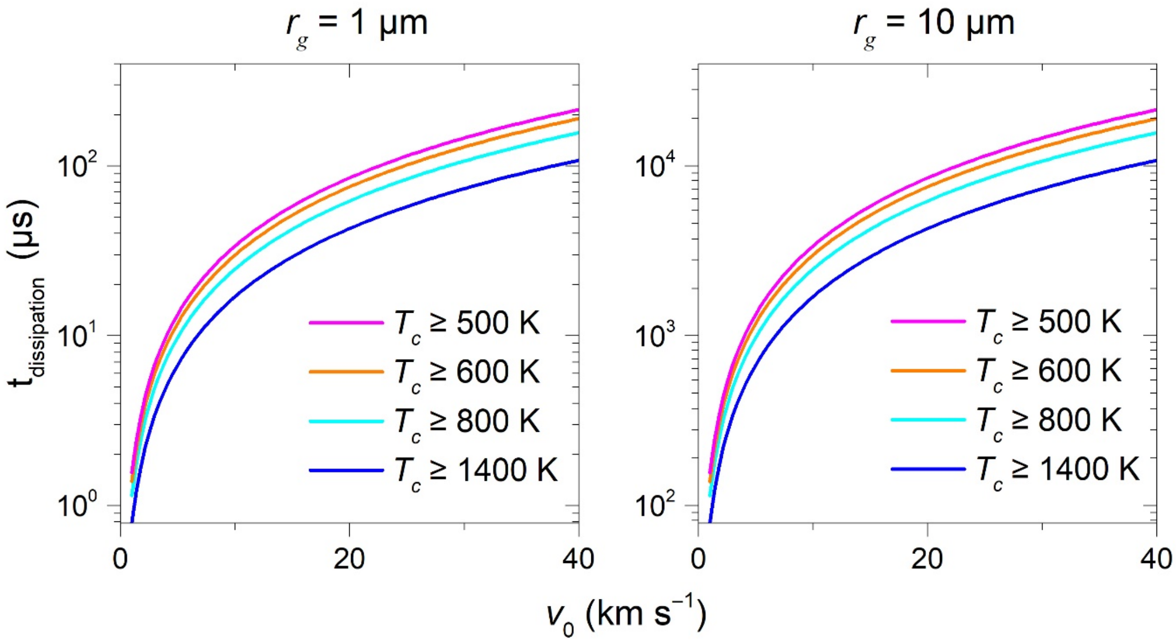

Supplementary Fig. 8. Timescales for crater thermal dissipation as a function of minimum temperature assumed for impact crater (r_g = projectile size, v_0 = impact velocity, and T_c = average temperature of crater). These timescales are comparable to the thermal dissipation timescales using material strength properties of the target material.

Supplementary Table 1 List of experiments

	Irradiation Temperature (K)	Irradiation source
1	5	Blank
2	5	Electron
3	5	Laser
4	5	Electron + Laser
5	150	Blank
6	150	Electron
7	150	Laser
8	150	Electron + Laser

Supplementary Table 2 Summary of the parameters for the space weathering of the Murchison meteorite.

	e^-	CO_2-laser	e^- and CO_2-laser	
			e^-	CO_2-laser
Initial energy of the electrons (keV)	5		5	
Electron current (μA)	10 ± 1		10 ± 1	
Irradiation time (min)	240[a]	300	300	300
Average penetration depth (μm)	0.14 ± 0.02		0.14 ± 0.02	
Dose per atomic mass unit (eV amu^{-1})	121 ± 24		151 ± 30	
Laser power (W cm^{-2})		8.0 ± 0.4		8.0 ± 0.4
Total deposited laser energy (J m^{-2})		$(1.44 \pm 0.16) \times 10^9$		$(1.44 \pm 0.16) \times 10^9$

[a]Due to a technical issue, the irradiation time is 60 minutes shorter than other experiments.

Supplementary Table 3 Calculated column densities (molecules cm^{-2}) of organics, carbon dioxide (CO_2), and water (H_2O) from IR and QMS data.

			IR				QMS	
	Band position[a]	Absorption coefficient[b]	5 K		150 K		TPD after irradiation at 5 K	TPD after irradiation at 150 K
			Before irradiation	After irradiation	Before irradiation	After irradiation		
Organics (in CH_2 units)	2955, 2922, 2848	3.8×10^{-18}[c]	$(1.0 \pm 0.2) \times 10^{16}$	$(0.4 \pm 0.1) \times 10^{15}$	$(1.0 \pm 0.2) \times 10^{16}$	$(0.1 \pm 0.0) \times 10^{15}$		
		2.0×10^{-19}[d]	$(1.9 \pm 0.4) \times 10^{17}$	$(0.9 \pm 0.2) \times 10^{17}$	$(2.0 \pm 0.4) \times 10^{17}$	$(0.2 \pm 0.1) \times 10^{17}$		
Carbon dioxide (CO_2)	2341	1.1×10^{-16}[d]	-	$(2.1 \pm 0.4) \times 10^{14}$	-	$(1.9 \pm 0.4) \times 10^{14}$	$(1.9 \pm 0.4) \times 10^{14}$	$(1.1 \pm 0.3) \times 10^{14}$
		7.6×10^{-17}[d]	-	$(2.8 \pm 0.6) \times 10^{14}$	-	$(2.6 \pm 0.6) \times 10^{14}$		
Water (H_2O)	3380	2.4×10^{-16}[d]	-	$(1.8 \pm 0.4) \times 10^{15}$	-	$(1.5 \pm 0.3) \times 10^{17}$	$(2.0 \pm 0.4) \times 10^{15}$	$(0.3 \pm 0.1) \times 10^{17}$

Notes:

[a]In cm^{-1}.

[b]In cm molecule^{-1}.

[c]Taken from Hudson *et al*., 2014[1].

[d]Taken from Bouilloud *et al*., 2015[2].

References

1 Hudson, R. L., Gerakines, P. A. & Moore, M. H. Infrared spectra and optical constants of astronomical ices: II. Ethane and ethylene. *Icarus* **243**, 148-157 (2014).

2 Bouilloud, M. *et al.* Bibliographic review and new measurements of the infrared band strengths of pure molecules at 25 K: H_2O, CO_2, CO, CH_4, NH_3, CH_3OH, HCOOH and H_2CO. *Mon. Not. Roy. Astron. Soc.* **451**, 2145-2160 (2015).